

Matlab/Simulink Modeling of Four-leg Voltage Source Inverter With Fundamental Inverter output Voltages Vector Observation

Riyadh G. Omar

Electrical Engineering Dept. College of
Engineering
University of Basra
Riy68gh@yahoo.com

Dr.Rabee' H. Thejel

Electrical Engineering Dept. College of
Engineering
University of Basra
Rabee_alabbasi@ieec.org

Abstract. Four-leg voltage source inverter is an evolution of the three-leg inverter, and was ought about by the need to handle the non-linear and unbalanced loads. In this work Matlab/ Simulink model is presented using space vector modulation technique. Simulation results for worst conditions of unbalanced linear and non-linear loads are obtained. Observation for the continuity of the fundamental inverter output voltages vector in stationary coordinate is detected for better performance. Matlab programs are executed in block functions to perform switching vector selection and space vector switching.

Index Terms— Four-leg inverter, large signal model, space vector pulse width modulation, nonzero-switching vector, zero-switching vector, non-linear load.

I. INTRODUCTION

Three-phase four-leg inverters have great interest in modern industrial applications, such as power generation, distributed stand-alone energy systems[1-4]. This inverter has its specialty because of the fourth-wire which connects the neutral to the load. Imbalance in the current drawn from each phase of the supply requires an extra neutral connection to deal with the zero sequence current which then results[5, 6]. Space vector modulation has proved to be one of the most popular and favorable pulse-width modulation schemes due to its high dc link voltage utilization, low output distortion, and ability to minimize the switching and conduction losses [7]. Recently different and more complex SVPWM methods have been developed for

multiphase machines and electric-vehicle applications[8, 9]. The goal of the three-phase four-leg inverter is to maintain the desired sinusoidal output voltage waveform over all loading conditions and transients. This is ideal for applications like data communication, industrial automation, military equipment, which require high performance UPS [10]. This work presents a comprehensive study of three-dimensional space vector modulation (3-DSVM) schemes for four-leg voltage-source inverter. Section II describes four-leg voltage-source inverter and its average large models, which can be used, with its control loop, to derive the reference voltage vector for SVM. In Section III 3-D space vectors are defined. Based on the definition, sixteen switching state vectors (SSVs) are plotted in the 3-D space. The adjacent switching vectors used to

arraying the reference vector are then identified using two-step procedure. A symmetrically aligned sequence scheme is presented.

II. FOUR-LEG VOLTAGE-SOURCE INVERTER TOPOLOGY

The schematic diagram of a four-leg inverter is shown in Fig.1. This topology is known to have balanced output voltages even under unbalanced load conditions. Due to the additional leg, a four-leg inverter can assume sixteen switching states, which is twice that in a conventional three-leg inverter.

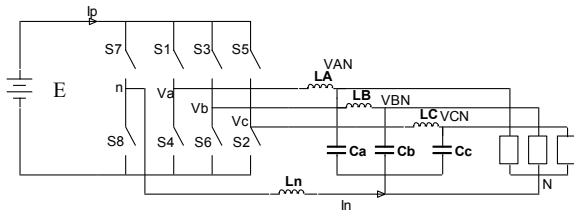


Fig.1 Four-leg inverter

A. Average Model of Four-Leg Voltage-Source Inverter

The large-signal average model of the four-leg voltage-source inverter is used to find the reference voltage vector for 3-D SVM in steady state, and for control loop design. They are obtained by replacing the four-leg switching network shown in Fig. 1 with its average model. With a pulse width modulation control, the ac terminal voltages, and the dc terminal current of the switching network are pulsating in a switching period. To calculate the average values in a switching period, the moving average operand is expressed in Eq. (1), for an arbitrary variable (X_t).

$$X_t = \frac{1}{T_s} \int_{t-T_s}^t X_\tau d\tau \quad (1)$$

After a cycle-by-cycle averaging process, the averaged ac terminal voltages, V_{an} , V_{bn} , and V_{cn} and the dc terminal current are expressed as

$$[V_{an} \ V_{bn} \ V_{cn}]^T = [d_{an} \ d_{bn} \ d_{cn}]^T \cdot E \quad (2)$$

$$I_p = [d_{an} \ d_{bn} \ d_{cn}] \cdot [I_a \ I_b \ I_c]^T \quad (3)$$

where: d_{an} , d_{bn} , and d_{cn} are line-to-neutral duty ratios[11]. According to Eqs. (2), and (3) the average large-signal circuit model of the four-legged switching network is shown in Fig.1. It is arranged by the four-leg switching network with the averaged switching network model. The large-signal average circuit model of the four-leg inverter given in a-b-c coordinate is shown in Fig.2. From this model one can have:

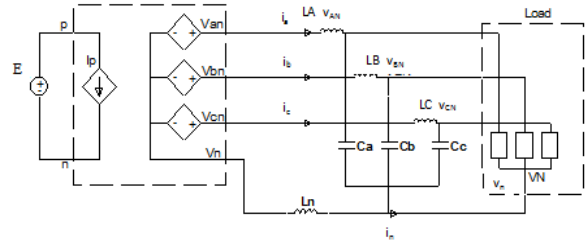


Fig.2 Average large signal model of four-leg inverter

$$\begin{bmatrix} V_{an} \\ V_{bn} \\ V_{cn} \end{bmatrix} = \begin{bmatrix} L \left(\frac{di_{LA}}{dt} + C \frac{d^2 V_{AN}}{dt^2} \right) + V_{AN} - L_n \frac{di_n}{dt} \\ L \left(\frac{di_{LB}}{dt} + C \frac{d^2 V_{BN}}{dt^2} \right) + V_{BN} - L_n \frac{di_n}{dt} \\ L \left(\frac{di_{LC}}{dt} + C \frac{d^2 V_{CN}}{dt^2} \right) + V_{CN} - L_n \frac{di_n}{dt} \end{bmatrix} \quad (4)$$

$$i_n = -(i_{LA} + i_{LB} + i_{LC}) - C \frac{d(V_{AN} + V_{BN} + V_{CN})}{dt} \quad (5)$$

where: i_{LA} , i_{LB} , and i_{LC} are three-phase load currents, and i_n is the neutral current.

Under the assumption of having known output three-phase voltages (balanced or not), the inverter output voltages which are used as the reference control voltages v_{an} , v_{bn} , and v_{cn} in the a-b-c coordinate can be calculated using Eqs. (4), and (5)[9].

B. Definition of 3-D SVPWM

In the four-leg inverter, the assumption of

$$X_a + X_b + X_c = 0$$

where X may be current or voltage is no longer need to be valid while the fact that

$$X_a + X_b + X_c \neq 0 \quad (6)$$

suggests that the three variables become truly independent, and can be represented by a vector (X) in 3-D orthogonal (α - β - γ) coordinate, where

$$X = X_\alpha + jX_\beta + kX_\gamma \quad (7)$$

The transformed voltages in the (α, β, γ) space can be obtained using the transformation

$$\begin{bmatrix} V_\alpha \\ V_\beta \\ V_\gamma \end{bmatrix} = T \begin{bmatrix} V_{an} \\ V_{bn} \\ V_{cn} \end{bmatrix}, T = \frac{2}{3} \begin{bmatrix} 1 & \frac{-1}{2} & \frac{-1}{2} \\ 0 & \frac{\sqrt{3}}{2} & \frac{-\sqrt{3}}{2} \\ \frac{1}{2} & \frac{1}{2} & \frac{1}{2} \end{bmatrix} \quad (8)$$

Applying Eq.(8) to the control reference voltage described in Eqs.(4), and (5) the reference voltage vector in the $(\alpha\text{-}\beta\text{-}\gamma)$ coordinate is obtained.

$$V_{ref} = \begin{bmatrix} V_{\alpha_ref} \\ V_{\beta_ref} \\ V_{\gamma_ref} \end{bmatrix} = \frac{2}{3} \begin{bmatrix} 1 & \frac{-1}{2} & \frac{-1}{2} \\ 0 & \frac{\sqrt{3}}{2} & \frac{-\sqrt{3}}{2} \\ \frac{1}{2} & \frac{1}{2} & \frac{1}{2} \end{bmatrix} \begin{bmatrix} V_{an_ref} \\ V_{bn_ref} \\ V_{cn_ref} \end{bmatrix} \quad (9)$$

In four-leg inverter there are sixteen different combination of switching states. Each of these switching states represents a certain space vector, while in a conventional three-leg inverter only eight switching states are seen. This means that four-leg inverter is double complicated than three-leg inverter. These sixteen switching states are listed in Table I, where (1) means that the upper switch in the leg is on and the lower switch is off, while (0) means that the upper switch in the leg is off and the lower switch is on. Applying the transformation given in Eq.(9), can be gained. The switching space vectors in (α, β, γ) coordinate are shown in Table II. It is clear from these tables that there are two zero switching vectors (1111, 0000) and fourteen nonzero switching vectors. These switching vectors are shown in Fig.3 (a). In the space of transformed phase voltages $\{v_\alpha, v_\beta, v_\gamma\}$, where α, β plane is the plane in which $v_{an} + v_{bn} + v_{cn} = 0$, and γ is the axis of the zero sequence component. The vertices of these vectors when projected onto the (α, β) plane would form a regular hexagon as shown in Fig.3 (b).

III. SYNTHESIS OF THE REFERENCE VECTOR

The reference vector (V_{ref}) is synthesized by using the switching vectors shown in Fig.3 in every switching cycle. This can be implemented by the following two steps:

(i) Selection of switching vectors.

(ii) Projection of the reference vector onto selected switching vectors.

Step 1: Switching vectors adjacent to the reference vector should be selected since the adjacent switching vectors produce non-conflicting voltage pulses (same voltage polarity). Step 2: Identification of the adjacent switching vectors for 3-D SVM which takes two steps, namely prism identification and tetrahedron identification.

Table-I Switching combinations and the four-leg switching network ac terminal voltages.

Vector	Leg a	Leg b	Leg c	Leg n	V_{an}	V_{bn}	V_{cn}
V_0	0	0	0	0	0	0	0
V_1	0	0	0	1	-E	-E	-E
V_2	0	0	1	0	0	0	E
V_3	0	0	1	1	-E	-E	0
V_4	0	1	0	0	0	E	0
V_5	0	1	0	1	-E	0	-E
V_6	0	1	1	0	0	E	E
V_7	0	1	1	1	-E	0	0
V_8	1	0	0	0	E	0	0
V_9	1	0	0	1	0	-E	-E
V_{10}	1	0	1	0	E	0	E
V_{11}	1	0	1	1	0	-E	0
V_{12}	1	1	0	0	E	E	0
V_{13}	1	1	0	1	0	0	-E
V_{14}	1	1	1	0	E	E	E
V_{15}	1	1	1	1	0	0	0

The prism identification is very similar to the sector identification for 2-D SVM. Based on the projections of the reference vector on the $(\alpha\text{-}\beta)$ plane V_α , and V_β , six prisms in the 3-D space can be identified and numbered as Prisms 1 through 6, and from here it is trivial to calculate the phase angle in this plane by using Eq.(10) below, which specifies which prism the output voltage vector lies within[12].

Table-II Switching combinations and inverter voltages in the α, β, γ coordinate.

Vec tor	Le g a	Le g b	Le g c	Leg n	V_α	V_β	V_γ
V_0	0	0	0	0	0	0	0
V_1	0	0	0	1	0	0	-E
V_2	0	0	1	0	$-\frac{1}{3}E$	$-\frac{1}{\sqrt{3}}E$	$\frac{1}{3}E$
V_3	0	0	1	1	$-\frac{1}{3}E$	$-\frac{1}{\sqrt{3}}E$	$-\frac{2}{3}E$
V_4	0	1	0	0	$-\frac{1}{3}E$	$\frac{1}{\sqrt{3}}E$	$\frac{1}{3}E$
V_5	0	1	0	1	$-\frac{1}{3}E$	$\frac{1}{\sqrt{3}}E$	$-\frac{2}{3}E$
V_6	0	1	1	0	$-\frac{2}{3}E$	0	$\frac{2}{3}E$
V_7	0	1	1	1	$-\frac{2}{3}E$	0	$-\frac{1}{3}E$
V_8	1	0	0	0	$\frac{2}{3}E$	0	$\frac{1}{3}E$
V_9	1	0	0	1	$\frac{2}{3}E$	0	$-\frac{2}{3}E$
V_{10}	1	0	1	0	$\frac{1}{3}E$	$-\frac{1}{\sqrt{3}}E$	$\frac{2}{3}E$
V_{11}	1	0	1	1	$\frac{1}{3}E$	$-\frac{1}{\sqrt{3}}E$	$-\frac{1}{3}E$
V_{12}	1	1	0	0	$\frac{1}{3}E$	$\frac{1}{\sqrt{3}}E$	$\frac{2}{3}E$
V_{13}	1	1	0	1	$\frac{1}{3}E$	$\frac{1}{\sqrt{3}}E$	$-\frac{1}{3}E$
V_{14}	1	1	1	0	0	0	E
V_{15}	1	1	1	1	0	0	0

$$\theta_{\alpha\beta} = \tan^{-1} \frac{V_{\beta_ref}}{V_{\alpha_ref}} \quad (11)$$

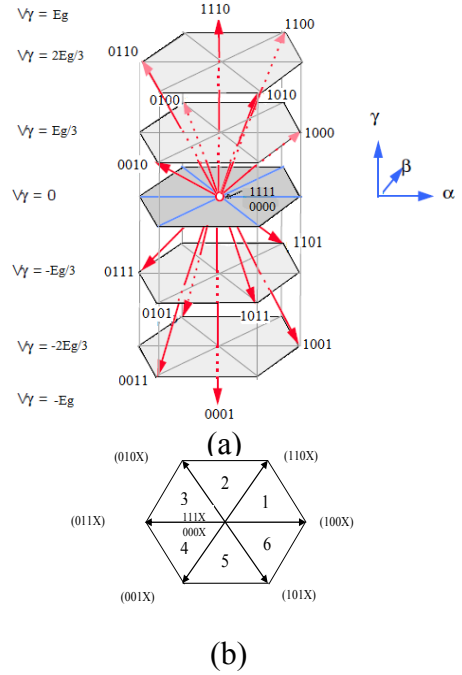


Fig.3 Switching vectors in α, β, γ coordinate. (a) Switching state vectors of a four-leg inverter. (b) Top view of the sixteen vectors into α, β plane.

IV. DETERMINATION OF TIME DURATION AND SEQUENCING OF THE SWITCHING VECTORS.

The time duration of the selected switching vectors can be computed by projecting the reference vector onto the adjacent NZSVs. This is illustrated for the case when the reference vector is in tetrahedron 2 (T2) in Fig.4, where the duty-cycles d_1, d_2, d_3 for the active vectors ‘V1=1000’, ‘V2=1001’, ‘V3=1101’ are obtained based on projections from the following:

$$V_{ref} = d_1 \cdot V_1 - d_2 \cdot V_2 - d_3 \cdot V_3 \quad (12)$$

$$\begin{bmatrix} d_1 \\ d_2 \\ d_3 \end{bmatrix} = \frac{1}{E} \begin{bmatrix} 1 & 0 & 1 \\ \frac{1}{2} & \frac{-\sqrt{3}}{2} & -1 \\ 0 & \sqrt{3} & 0 \end{bmatrix} \begin{bmatrix} V_{\alpha_ref} \\ V_{\beta_ref} \\ V_{\gamma_ref} \end{bmatrix} \quad (13)$$

$$d_0 = 1 - d_1 - d_2 - d_3 \quad (14)$$

$$\text{prism No.} = \begin{cases} 1 & \text{for } 0 \leq \theta_{\alpha\beta} < \frac{\pi}{3} \\ 2 & \text{for } \frac{\pi}{3} \leq \theta_{\alpha\beta} < \frac{2\pi}{3} \\ 3 & \text{for } \frac{2\pi}{3} \leq \theta_{\alpha\beta} < \pi \\ 4 & \text{for } \pi \leq \theta_{\alpha\beta} < \frac{4\pi}{3} \\ 5 & \text{for } \frac{4\pi}{3} \leq \theta_{\alpha\beta} < \frac{5\pi}{3} \\ 6 & \text{for } \frac{5\pi}{3} \leq \theta_{\alpha\beta} < 2\pi \end{cases} \quad (10)$$

where, $\theta_{\alpha\beta}$ is the phase angle of the output voltage in the $(\alpha-\beta)$ plane. The value of $\theta_{\alpha\beta}$ given in Eq. (10) can be calculated as

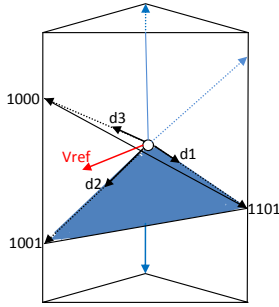


Fig.4 Duty cycles for the active vectors in T2.

The complete table for the corresponding NZSVs and projection matrices to compute the duty ratios for all 24 tetrahedrons is shown in Appendix B. The selection of ZSVs and the sequencing of switching vectors involve trade-off between switching losses and harmonic distortion; symmetrically aligned sequence of switching vectors is used in this work as shown in Fig.5. Finally to describe the inverter output voltages and the dc terminal current of the four-leg inverter switching network, as in Eqs.(2), and (3) a switching function is defined in Eq.(15).

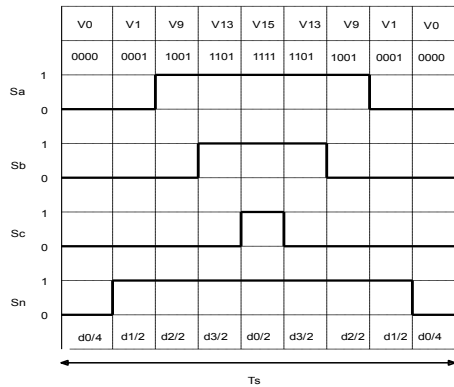


Fig.5 symmetrically aligned sequence (pattern) for tetrahedron T1.

$$\begin{aligned}
 d_{an} &= \left\{ \begin{array}{l} 1 \text{ if } S_1 \text{ and } S_8 \text{ are closed} \\ 0 \text{ if } S_4 \text{ and } S_8 \text{ or } S_1 \text{ and } S_7 \text{ are closed} \\ -1 \text{ if } S_4 \text{ and } S_7 \text{ are closed} \end{array} \right\} \\
 d_{bn} &= \left\{ \begin{array}{l} 1 \text{ if } S_3 \text{ and } S_8 \text{ are closed} \\ 0 \text{ if } S_6 \text{ and } S_8 \text{ or } S_3 \text{ and } S_7 \text{ are closed} \\ -1 \text{ if } S_6 \text{ and } S_7 \text{ are closed} \end{array} \right\} \\
 d_{cn} &= \left\{ \begin{array}{l} 1 \text{ if } S_5 \text{ and } S_8 \text{ are closed} \\ 0 \text{ if } S_2 \text{ and } S_8 \text{ or } S_5 \text{ and } S_7 \text{ are closed} \\ -1 \text{ if } S_2 \text{ and } S_7 \text{ are closed} \end{array} \right\}
 \end{aligned} \quad (15)$$

V. MATLAB/SIMULINK MODELING OF THE THREE-PHASE FOUR-LEG VOLTAGE SOURCE INVERTER.

A Matlab/Simulink software package model for the generation of the inverter switching pulses is constructed, using average large signal model (Eqs. (4), (5), and (8-15)) of the inverter to produce a reference vector in the (α-β-γ) plane. Identification process is implemented to determine the number of prism and tetrahedron that locates the position of the reference vector. Using the symmetrically aligned switching sequence pattern of the 6 prisms, 24 tetrahedrons duty time ratios for each switching vector is calculated. This model is shown in Fig.6.

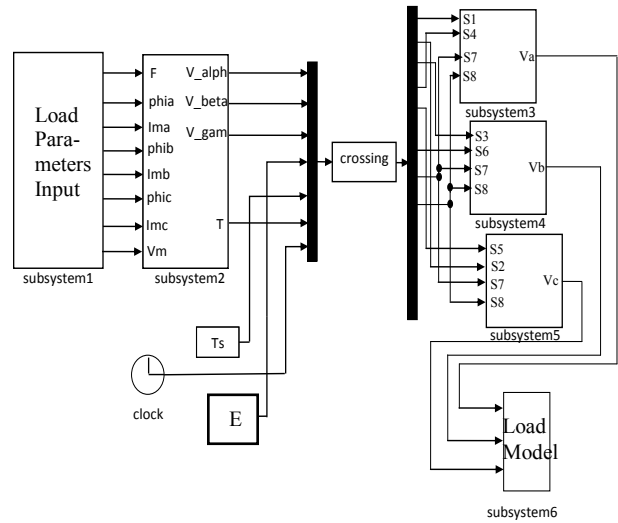


Fig.6 Matlab/Simulink model for system simulation.

Subsystem-1 contains the load currents, frequency, and three-phase command voltages. Subsystem-2 calculates the three-phase reference voltages in (a-b-c) and (α-β-γ) planes. This subsystem uses a Matlab/Simulink S-function blocks to identify the number of prism and tetrahedron which locates the reference vector position in whole simulation period. The information obtained from subsystem-2 with D.C source voltage and switching time (Ts) are the input data to a Matlab M-file program (crossing S-function block) which computes the phase leg duty ratios in a line cycle according to the symmetrical switching sequence pattern shown in Fig.6. The flow chart of this program for the first leg is shown in Fig.7. Subsystems-(3-5) applying

Eqs.(2), and (15) to produce inverter three-phase output voltage pulses. Subsystem-6 represents the low-pass filter and load parameters. The three-phase load terminal voltages, load currents, neutral current, trajectory of the fundamental inverter output voltages, THD, and frequency response can be monitored in this subsystem.

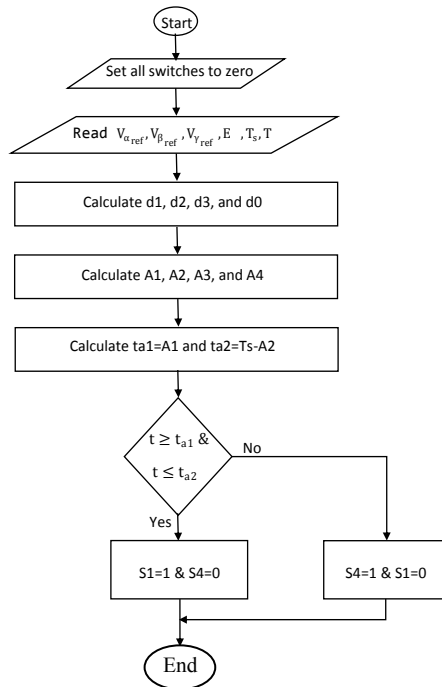


Fig.7 Crossing S-function program flow chart for the first leg.

VI. SIMULATION RESULTS

Simulation is performed for the four-leg SVPWM inverter by using Matlab/Simulink software package program to justify the validity and the efficiency of the model performance for unbalanced load. Worst case of unbalance loads (resistive in phase a, capacitive in phase b, and inductive in phase c) are used with $I_A=180\angle 0$, $I_B=90\angle -90$ and $I_C=90\angle -240$ A. also to confirm the results, simulation is repeated with non-linear load consists of three two-leg uncontrolled rectifiers supplying 14.14Ω, 15.71Ω, and 17.67Ω loads. Inverter parameters used in simulation are shown in Appendix A. The simulation results are listed through Figs.8-22. Figure 8 shows the comparisons between the reference command voltages and inverter output voltages. This figure proves the ability of the model to follow the

reference command voltage almost completely. Figure 9 shows the trajectory of the fundamental inverter output voltages vector in $(\alpha-\beta-\gamma)$ plane. This trajectory takes ellipse shape in 3-D compared with 2-D circle shape in conventional three-leg inverter. Observation of this trajectory indicates the continuity of the reference space voltage vector which is good for better space vectors switching performance. In Fig.10 the duty phase ratios computed in the Matlab M-file program for each inverter leg which corresponds to symmetrically sequence pattern. Figure 11 shows the unbalanced load currents. In Fig.12 balanced load terminals voltages for the unbalanced load currents are shown which confirm the benefits of this type of inverters. Figure 13 shows the neutral current under unbalance load conditions. Figure 14 shows the relation between the THD computed for the inverter output voltages against various modulation index. Figures 15-17 show the three phase inverter output voltages, inverter load currents, and neutral current before (LC) filter stage and neutral inductor respectively. Figure 18 shows the inverter three phase balanced output load voltages for non-linear load, which consists of three unbalanced two-leg uncontrolled rectifiers. Figure 19 shows inverter unbalanced load currents with non-linear three unbalanced two-leg uncontrolled rectifiers. Figure 20 shows the neutral current for that type of loads. Figures 21 and 22 showing the non-linear rectifier load output voltages and currents respectively. These results confirm the important features of the four-leg SVPWM inverter with various types of loads.

VII. CONCLUSION

In this paper Matlab/Simulink model for four-leg space vector pulse width modulation inverter with average large signal inverter model is proposed with symmetrically aligned sequence switching schem, the most important factors in 3D-SVPWM analyzed using different types of load (linear and non-linear). All the results show the advantages of this type of inverters and its ability to handle unbalance loads, and neutral current through the fourth leg with its connection

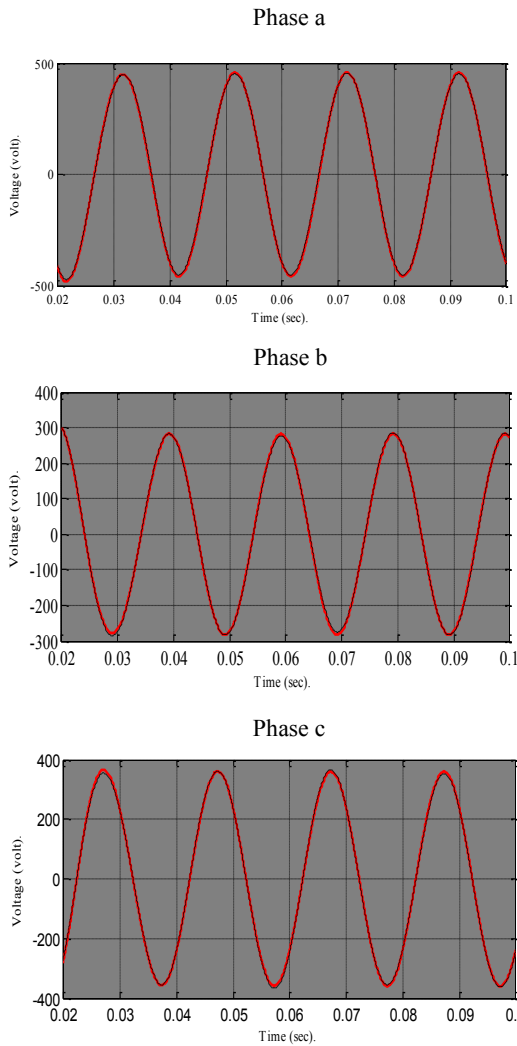


Fig.8 Comparison between reference command voltages (red line) and inverter output voltages (black line).

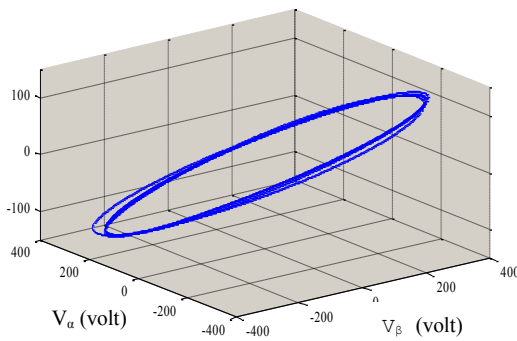


Fig9. Trajectory of the fundamental inverter output voltages vector in $(\alpha-\beta-\gamma)$ plane.

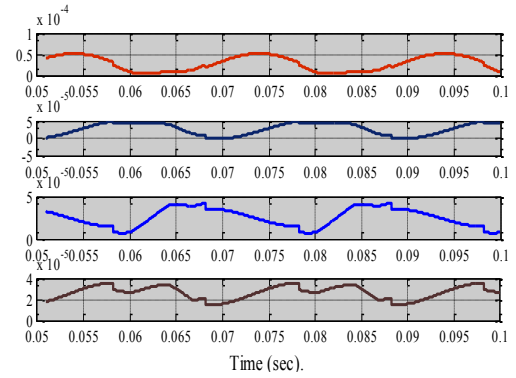


Fig10. Phase leg duty ratios.

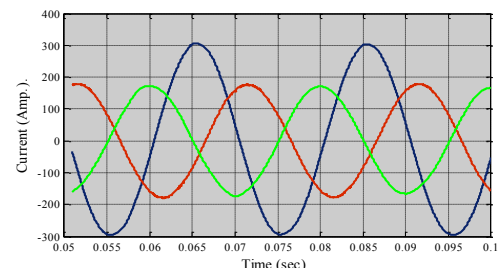


Fig.11 Three-phase load currents.

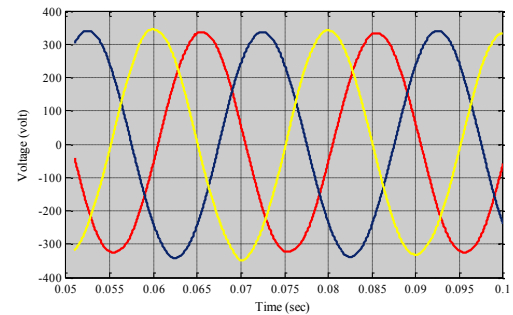


Fig.12 Three-phase load terminal voltages.

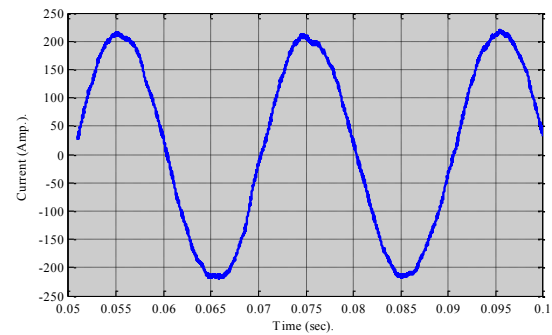


Fig.13 Neutral current

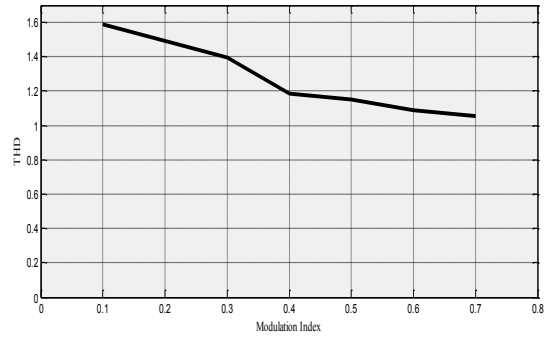


Fig.14 Inverter output voltage THD versus modulation index.

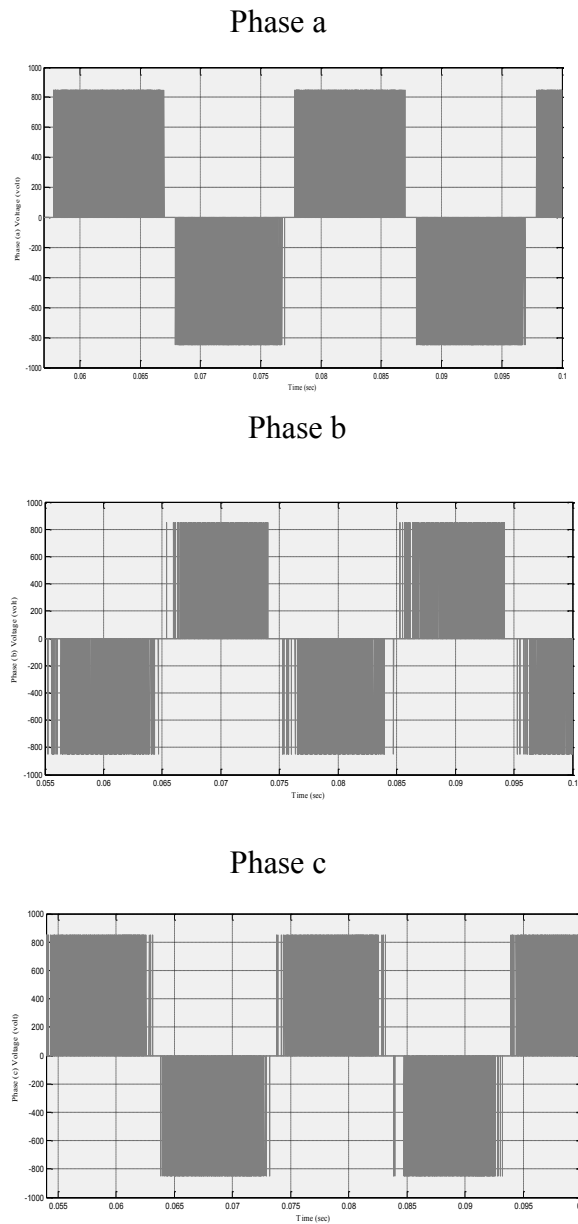


Fig.15 Inverter output phase voltages

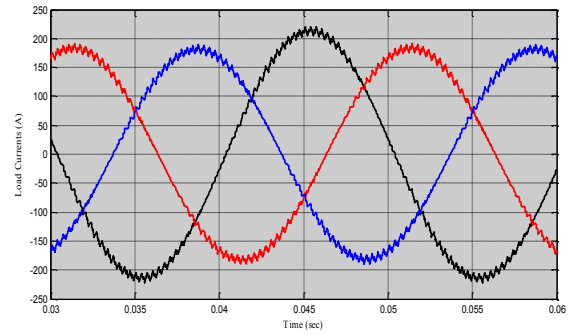


Fig.16 Inverter output currents before filter stage.

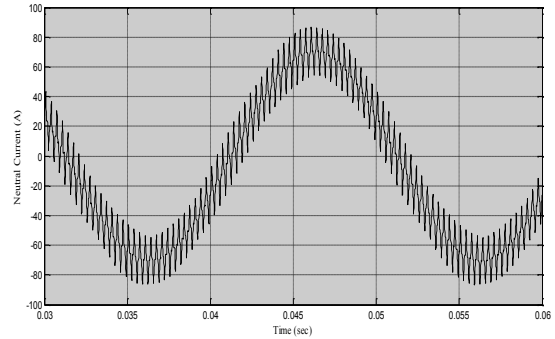


Fig.17 Inverter neutral current before neutral Inductor.

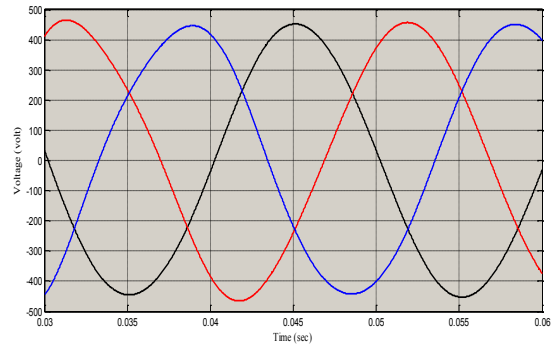


Fig.18 Inverter output voltages with non-linear load of three (two-leg) uncontrolled rectifiers

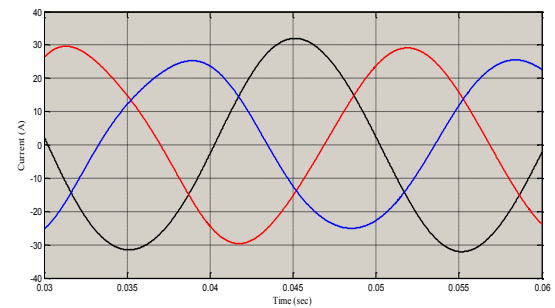


Fig.19 Inverter load currents with non-linear load of three (two-leg) uncontrolled rectifiers.

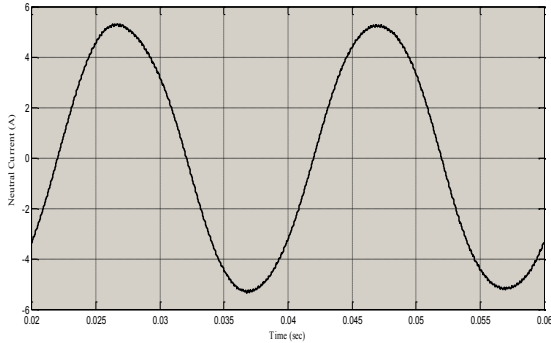


Fig.20 Neutral current for non-linear load

to load neutral point. Continuity of the fundamental inverter output voltages vector in (α - β - γ) plane is detected as a new approach, which represents a good indication for better SVPWM performance. Comparison between reference command voltages and inverter output voltages is performed to detect any deviation; the results show that these two signals are almost identical. Inverter output voltage THD is calculated with different modulation index for unbalance load conditions, the results give acceptable values with symmetrically aligned sequence switching schem.

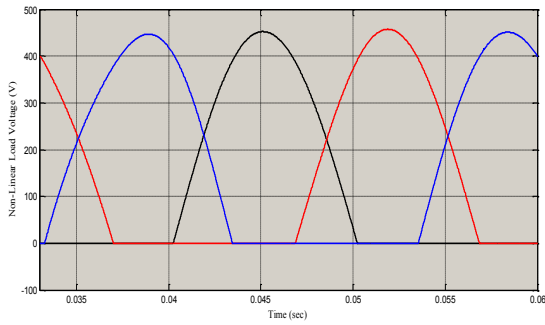


Fig.21 non-linear load (rectifier) output voltages

APPENDIX A

Circuit parameters

- (1) Dc link voltage: $E_g=850V$,
- (2) Filter capacitor: $C=400\mu F$,
- (3) Filter inductor: $L=3.5mH$,
- (4) Neutral inductor: $L_n=0.3mH$,
- (5) Switching frequency: 10 KHz.

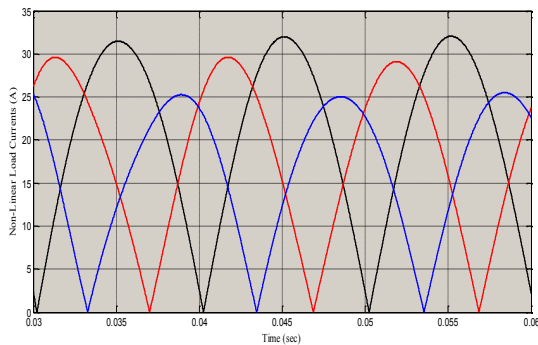


Fig.22 non-linear load (rectifier) output currents

APPENDIX B

Pr.	Tetrahedron			
1	T1 Van,Vbn,Vcn(-, -, -) V1,V9,V13 $\begin{bmatrix} -1 & 0 & -1 \\ \frac{3}{2} & \frac{-\sqrt{3}}{2} & 0 \\ 0 & \sqrt{3} & 0 \end{bmatrix}$	T2 Van,Vbn,Vcn(+, -, -) V8,V9,V13 $\begin{bmatrix} 1 & 0 & 1 \\ \frac{1}{2} & \frac{-\sqrt{3}}{2} & -1 \\ 0 & \sqrt{3} & 0 \end{bmatrix}$	T3 Van,Vbn,Vcn(+, +, -) V8,V12,V13 $\begin{bmatrix} \frac{3}{2} & \frac{-\sqrt{3}}{2} & 0 \\ \frac{-1}{2} & \frac{\sqrt{3}}{2} & 1 \\ \frac{1}{2} & \frac{\sqrt{3}}{2} & -1 \end{bmatrix}$	T4 Van,Vbn,Vcn(+, +, +) V8,V12,V14 $\begin{bmatrix} \frac{3}{2} & \frac{-\sqrt{3}}{2} & 0 \\ 0 & \sqrt{3} & 0 \\ \frac{-1}{2} & \frac{-\sqrt{3}}{2} & 1 \end{bmatrix}$
2	T5 Van,Vbn,Vcn(-, -, -) V1,V5,V13 $\begin{bmatrix} \frac{1}{2} & \frac{-\sqrt{3}}{2} & -1 \\ \frac{-3}{2} & \frac{\sqrt{3}}{2} & 0 \\ \frac{3}{2} & \frac{\sqrt{3}}{2} & 0 \end{bmatrix}$	T6 Van,Vbn,Vcn(-, +, -) V4,V5,V13 $\begin{bmatrix} \frac{-1}{2} & \frac{\sqrt{3}}{2} & 1 \\ -1 & 0 & -1 \\ \frac{3}{2} & \frac{\sqrt{3}}{2} & 0 \end{bmatrix}$	T7 Van,Vbn,Vcn(+, +, -) V4,V12,V13 $\begin{bmatrix} \frac{-3}{2} & \frac{\sqrt{3}}{2} & 0 \\ 1 & 0 & 1 \\ \frac{1}{2} & \frac{\sqrt{3}}{2} & -1 \end{bmatrix}$	T8 Van,Vbn,Vcn(+, +, +) V4,V12,V14 $\begin{bmatrix} \frac{-3}{2} & \frac{\sqrt{3}}{2} & 0 \\ \frac{3}{2} & \frac{\sqrt{3}}{2} & 0 \\ \frac{-1}{2} & \frac{-\sqrt{3}}{2} & 1 \end{bmatrix}$
3	T9 Van,Vbn,Vcn(-, -, -) V1,V5,V7 $\begin{bmatrix} \frac{1}{2} & \frac{-\sqrt{3}}{2} & -1 \\ 0 & \sqrt{3} & 0 \\ \frac{-3}{2} & \frac{-\sqrt{3}}{2} & 0 \end{bmatrix}$	T10 Van,Vbn,Vcn(-, +, -) V4,V5,V7 $\begin{bmatrix} \frac{-1}{2} & \frac{\sqrt{3}}{2} & 1 \\ \frac{1}{2} & \frac{\sqrt{3}}{2} & -1 \\ \frac{-3}{2} & \frac{-\sqrt{3}}{2} & 0 \end{bmatrix}$	T11 Van,Vbn,Vcn(-, +, +) V4,V6,V7 $\begin{bmatrix} 0 & \sqrt{3} & 0 \\ \frac{-1}{2} & \frac{-\sqrt{3}}{2} & 1 \\ -1 & 0 & -1 \end{bmatrix}$	T12 Van,Vbn,Vcn(+, +, +) V4,V6,V14 $\begin{bmatrix} 0 & \sqrt{3} & 0 \\ \frac{-3}{2} & \frac{-\sqrt{3}}{2} & 0 \\ 1 & 0 & 1 \end{bmatrix}$
4	T13 Van,Vbn,Vcn(-, -, -) V1,V3,V7 $\begin{bmatrix} \frac{1}{2} & \frac{\sqrt{3}}{2} & -1 \\ 0 & -\sqrt{3} & 0 \\ \frac{-3}{2} & \frac{\sqrt{3}}{2} & 0 \end{bmatrix}$	T14 Van,Vbn,Vcn(-, -, +) V2,V3,V7 $\begin{bmatrix} \frac{-1}{2} & \frac{-\sqrt{3}}{2} & 1 \\ \frac{1}{2} & \frac{-\sqrt{3}}{2} & -1 \\ \frac{-3}{2} & \frac{\sqrt{3}}{2} & 0 \end{bmatrix}$	T15 Van,Vbn,Vcn(-, +, +) V2,V6,V7 $\begin{bmatrix} 0 & -\sqrt{3} & 0 \\ \frac{-1}{2} & \frac{\sqrt{3}}{2} & 1 \\ -1 & 0 & -1 \end{bmatrix}$	T16 Van,Vbn,Vcn(+, +, +) V2,V6,V14 $\begin{bmatrix} 0 & -\sqrt{3} & 0 \\ \frac{-3}{2} & \frac{\sqrt{3}}{2} & 0 \\ 1 & 0 & 1 \end{bmatrix}$
5	T17 Van,Vbn,Vcn(-, -, -) V1,V3,V11 $\begin{bmatrix} \frac{1}{2} & \frac{\sqrt{3}}{2} & -1 \\ \frac{-3}{2} & \frac{-\sqrt{3}}{2} & 0 \\ \frac{3}{2} & \frac{-\sqrt{3}}{2} & 0 \end{bmatrix}$	T18 Van,Vbn,Vcn(-, -, +) V2,V3,V11 $\begin{bmatrix} \frac{-1}{2} & \frac{-\sqrt{3}}{2} & 1 \\ -1 & 0 & -1 \\ \frac{3}{2} & \frac{-\sqrt{3}}{2} & 0 \end{bmatrix}$	T19 Van,Vbn,Vcn(+, -, -) V2,V10,V11 $\begin{bmatrix} \frac{-3}{2} & \frac{-\sqrt{3}}{2} & 0 \\ 1 & 0 & 1 \\ \frac{1}{2} & \frac{-\sqrt{3}}{2} & -1 \end{bmatrix}$	T20 Van,Vbn,Vcn(+, +, +) V2,V10,V14 $\begin{bmatrix} \frac{-3}{2} & \frac{-\sqrt{3}}{2} & 0 \\ \frac{3}{2} & \frac{-\sqrt{3}}{2} & 0 \\ \frac{-1}{2} & \frac{\sqrt{3}}{2} & 1 \end{bmatrix}$
6	T21 Van,Vbn,Vcn(-, -, -) V1,V9,V11 $\begin{bmatrix} -1 & 0 & -1 \\ \frac{3}{2} & \frac{\sqrt{3}}{2} & 0 \\ 0 & -\sqrt{3} & 0 \end{bmatrix}$	T22 Van,Vbn,Vcn(+, -, -) V8,V9,V11 $\begin{bmatrix} 1 & 0 & 1 \\ \frac{1}{2} & \frac{\sqrt{3}}{2} & -1 \\ 0 & -\sqrt{3} & 0 \end{bmatrix}$	T23 Van,Vbn,Vcn(+, -, +) V8,V10,V11 $\begin{bmatrix} \frac{3}{2} & \frac{\sqrt{3}}{2} & 0 \\ \frac{-1}{2} & \frac{-\sqrt{3}}{2} & 1 \\ \frac{1}{2} & \frac{-\sqrt{3}}{2} & -1 \end{bmatrix}$	T24 Van,Vbn,Vcn(+, +, +) V8,V10,V14 $\begin{bmatrix} \frac{3}{2} & \frac{\sqrt{3}}{2} & 0 \\ 0 & -\sqrt{3} & 0 \\ \frac{-1}{2} & \frac{\sqrt{3}}{2} & 1 \end{bmatrix}$

References

- [1] Vechiu, I., Curea, O., Camblong, H. "Transient operation of a four-leg inverter for autonomous applications with unbalanced load" *IEEE Trans. Power Electron.*, Vol.25, No.2, Feb. 2010.
- [2] Yunwei, L., Vilathgamuwa, D.M., and Chiang, L.P. "Microgrid power quality enhancement using a three-phase four-wire grid-interfacing compensator" *IEEE Trans. Power Electron.*, Vol.19, No.1, pp.1707-1719, Nov./Dec. 2005.
- [3] Senjyu, T., Nakaji, T., Uezato, K., and Funabashi, T. "A hybrid power system using alternative energy facilities in isolated island" *IEEE Trans. Energy Convers.*, Vol.21, No.2, pp.406-414, Jun. 2005.
- [4] Marwali, M.N., Min, D., and Keyhani, A. "Robust stability analysis of voltage and current control for distributed generation systems" *IEEE Trans. Energy Convers.*, Vol.21, No.2, pp.516-526, Jun. 2006.
- [5] Ali, S.M., Kazmierkowski, M.P. "PWM voltage and current control of four-leg VSI" *Conf. Rec. of IEEE APEC 1998*.
- [6] Fraser, M.E., Manning, C.D., and Wells, B.M. "Transformerless four-wire PWM rectifier and its application in ac-dc-ac converters" *Electric Power Applications, IEE Proceedings*, Vol.142(6):pp.410-416, publication year 1995.
- [7] Zhang, R., Boroyevich, D., Prasad, V.H., Mao, H.C., Lee, F.C., and Dubovsky, S. "A three-phase inverter with a neutral leg with space vector modulation". In *Proc. IEEE APEC'97*, volume 2, pp.857-863, Feb.1997.
- [8] Duran, M. J., Prieto, J. F., Barrero, F., and Riveros, J. "Space-Vector PWM With Reduced Common-Mode Voltage for Five-Phase Induction Motor Drives". *IEEE Trans. Industrial Electronics.*, (vol.60, Issue10), Oct. 2013.
- [9] Abdelfatah, K., Bethoux, O. and DeBernardinis, A. "Space Vector PWM Control Synthesis for a H-Bridge Drive in Electric Vehicles". *IEEE Trans. Vehicular Technology.*, (vol.62), Jul. 2013.
- [10] Thandi, G. S. "Modeling Control and Stability of a PEBB based dc distribution power System". Master of science in Electrical Engineering theses. Virginia Polytechnic Institute and state University 1997.
- [11] Mason, N.J. "Modulation of a 4-leg matrix converter". PhD. theses Nottingham University, Nov.2011.
- [12] Zhang, R., Prasad, V.H., Boroyevich, D., and Lee, F.C. "Three dimensional space vector modulation for four-leg voltage-source converter". *IEEE Trans. Power Electron.*, 17(3):314-326, May 2002.